Earthquake Geotechnical Engineering for Protection and Development of Environment and Constructions – Silvestri & Moraci (Eds)
© 2019 Associazione Geotecnica Italiana, Rome, Italy, ISBN 978-0-367-14328-2

Application of SfM technique for measuring near-field earthquake-induced failures; case studies from Greece

S. Valkaniotis
Koronidos 9, Trikala, Greece

G. Papathanassiou
Department of Civil Engineering, Democritus University of Thrace, Greece

A. Ganas
Institute of Geodynamics, National Observatory of Athens

ABSTRACT: One of the main issues that a post-earthquake field survey must address is reporting the failures induced by the seismic event. However, it is well known that mapping these features is not always feasible due to several factors e.g. near-vertical slopes, coastall cliffs, high risk to human surveys. In order to overcome this issue and to quantitatively describe the earthquake-induced geological failures e.g. landslides and liquefaction-induced lateral spreading, remote sensing techniques were applied during the last decades such as Interferometric Synthetic Aperture Radar (InSAR), Light Detection and Ranging (LiDAR) and photogrammetric surveys. The latter one, a photogrammetric survey, is frequently conducted by use of Unmanned Aerial Vehicles (UAV), such as multicopters equipped with webcams, digital cameras and other sensors. The images acquired by the UAV can be processed using the Structure from Motion (SfM) image technique, thus providing a 3D point cloud. This study presents the application of the SfM approach in two post-earthquake UAV & field surveys conducted in Greece (Lefkada and Kos islands) for reporting the triggering of a deep-seated landslide and a lateral spreading case study, respectively.

1 INTRODUCTION

Documentation of earthquake environmental effects (surface ruptures, landslides etc.) is a very critical issue, since based on the accuracy of the provided information, protection and mitigation measures can be designed. UAVs provide a convenient remote sensing platform for post-earthquake surveys given their ability to collect ultra-high-resolution imagery in short time over terrain that is often difficult to access. Using the Structure from Motion (SfM) image processing technique, a 3D point cloud can be created by intersecting the matched features between the overlapping, offset images. Point clouds from optical images enable detailed representation of complex 3D surfaces, better editing and classification of the dataset and creation of further products like orthophotos, DSMs, DTMs, textured models etc. Comparison between different point cloud sets enables highly accurate change detection analysis, using recently developed matching algorithms. This work presents the mapping of earthquake-induced failures from two strong and shallow earthquakes occurred on November 17, 2015 (Mw 6.5) and July 20, 2017 (Mw 6.6) at the island of Lefkada, Ionian Sea and at the island of Kos, Aegean Sea, Greece. In the latter case, the SfM-based technique was applied using a ground-based digital camera, while in the former one a UAV DJI Phantom 3 was used. The Lefkada case study focuses on a deep-seated landslide triggered at the coastal area of Okeanos, SW Lefkada that induced severe damages to a recently constructed luxury hotel, while the Kos case study deals with the lateral spreading reported in the old harbor of the city.

The results validate the usefulness and accuracy of SfM technique for low cost and rapid documenting and mapping earthquake environmental effects. The accuracy and detail achieved is sufficient for most geological applications, even without the use of survey-grade ground control points.

2 CASE STUDY OF 2015 LEFKADA, GREECE EARTHQUAKE

The November 17, 2015 Lefkada earthquake with a magnitude of Mw 6.5 (Ganas et al. 2016, Papathanassiou et al. 2017) was located onshore the southwestern part of Lefkada island. Rupture took place along a near-vertical strike-slip fault with dextral sense of motion with a strike of N20±5°E and dip to east with an angle of about 70-80 degrees that is part of the Cephalonia Transform fault zone. The majority of earthquake-induced geological effects were slope failures and particularly, rock falls and slides, and shallow and deep-seated landslides at the western coastal part of the island as well as at its central area, on both natural as well as cut slopes (Papathanassiou et al. 2017). The Okeanos landslide (Figure 1B) occurred at the western coast of Lefkada below a touristic residential site (Okeanos villas complex), about 2 km southwest of Athani village (Valkaniotis et al. 2018). Geologic formations in the site of the landslide are Quaternary scree and debris, with underlying Mesozoic limestones. The steep coastal cliff and the presence of fault discontinuities increase the landslide susceptibility of the area. The presence of an older inactive landslide in the site was discovered by examining the detailed topography of the area and historical aerial imagery.

In order to investigate the Okeanos landslide, a post-earthquake field survey was performed using a DJI Phantom 3 UAV. 75 images were acquired, covering the landslide area with both vertical and oblique views. Images were processed using the Agisoft Photoscan software, resulting in a point cloud of 24 million points. A detailed digital surface model (DSM) with pixel dimensions 0.08 m of an orthophoto map of similar pixel size were produced from the point cloud dataset. A stereo pair of aerial images (1:8000 scale, acquired in 2004) of the site was scanned and processed with Agisoft Photoscan, resulting in a 10 million point cloud used as a reference dataset.

Using the point cloud, digital surface model and orthophoto of the Okeanos site, the landslide extent was mapped in detail. Using both co-registered point clouds, we extracted profiles along the landslide site in order to measure the morphological changes and displacement. The landslide area covers a horizontal surface of ~36000 m^2 and the main body comprises a block sliding towards the coast from the Okeanos terrace at 240 m elevation a.s.l. The main slide caused a retreat of the cliff for 45-50 m towards east and is believed to have been initiated by slip along a

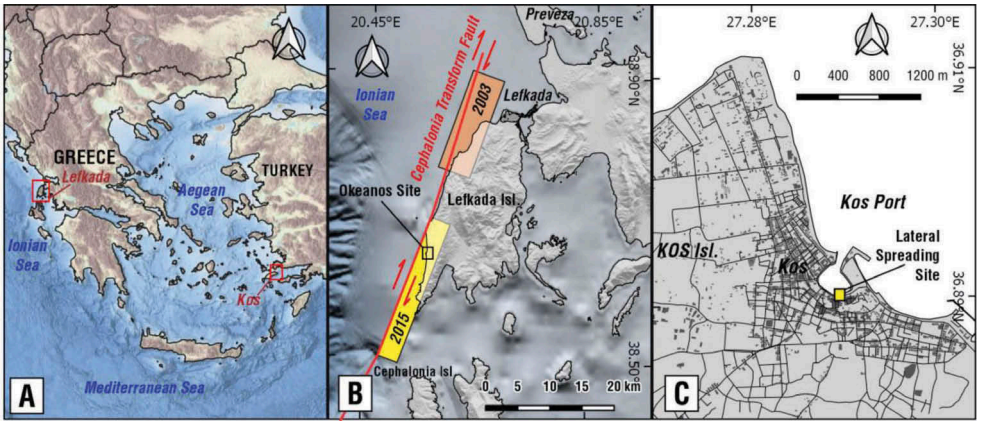

Figure 1. A) Overview map showing the location of the two case study sites. B) Lefkada island with the location of the Okeanos landslide site. The 2015 earthquake rupture is shown with a yellow polygon. C) Kos city map with the location of the lateral spreading site.

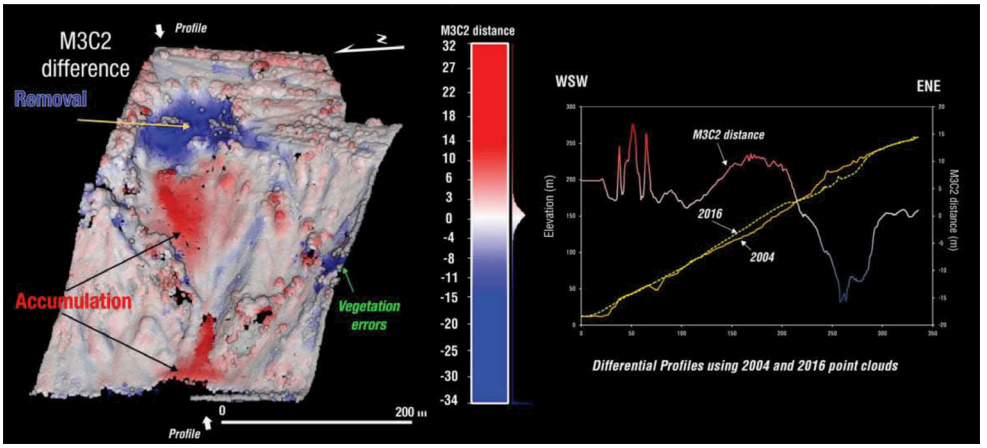

Figure 2. Left: Difference analysis between the two point clouds (2004 & 2016) after applying the M3C2 method. Blue indicates removed (volume loss) and red deposited material (volume gain), respectively. Right: Profiles along the landslide showing the difference in the surface between 2004 and 2016. Graduated Colour line depicts the M3C2 difference in meters along the profile; removed material at the top part of the landslide, and deposited material downslope.

Figure 2b. Deep-seated landslide in the area of Okeanos triggered by the 2015 earthquake. Image captured by UAV.

pre-existing fault surface. This surface was exposed after the landslide with a visible scarp at 20-25 m height. Removed material from the landslide was deposited downslope. Although the landslide scarp ends north of the villa complexes area, secondary sliding phenomena removed part of the Okeanos complex service road and created an undercutting at the western villa complex.

For the volumetric change analysis, the two point clouds were co-registered and compared using the M3C2 code (Multiscale Model to Model Cloud Comparison; Lague et al., 2013). A volume of ~93000 m^3 was calculated from differencing the two models (Valkaniotis et al. 2018). The differential map clearly marks the removed slide on the upper part of the cliff, the removed

area in the corner of the villa complexes as well as smaller secondary landslides in the cliff below the villa complexes and the deposited material in the bottom of the cliff (Figure 2).

To the north of Okeanos villas, an exposed slip surface at the head crown scarp of Okeanos landslide was surveyed as well. The exposed surface corresponds to a pre-existing fault surface dipping west that is divided in two parts of different orientation. The northern sub-fault plane (Plane 1) has a roughly NW-SE orientation and the southern sub-fault plane (Plane 2) has a roughly NNE-SSW orientation. Plane 2 is interpreted as the main slip surface, corresponding to a pre-existing fault plane antithetic, while Plane 1 is interpreted as either a secondary fault plane perpendicular to Plane 2 or a local curvature feature of the main Plane 2. Analysis was made using the qFacets plugin (Dewez et al., 2016) of CloudCompare software that enables automatic extraction of planar facets from point clouds and calculates their orientation and (orthogonal) distance. In particular, qFacets uses two algorithms to extract planar facets, *kd-tree* (Kd) that recursively divides the cloud in small planar patches, and *Fast Marching* (FM) that systematically divides the input point cloud in smaller patches and then regroups them with a (Fast Marching) front propagation. The results of both methods are shown in Figure 3, as stereonet lower-hemisphere projections, and rose diagrams. Plane 1 has a mean strike of N165° E and a dip of 56°, while Plane 2 has a mean strike of N203° E and a dip of 58°. The results are almost identical for both methods, possibly due to the clear exposure and small variation along the two surfaces. Orientation of the two fault sub-planes could explain a

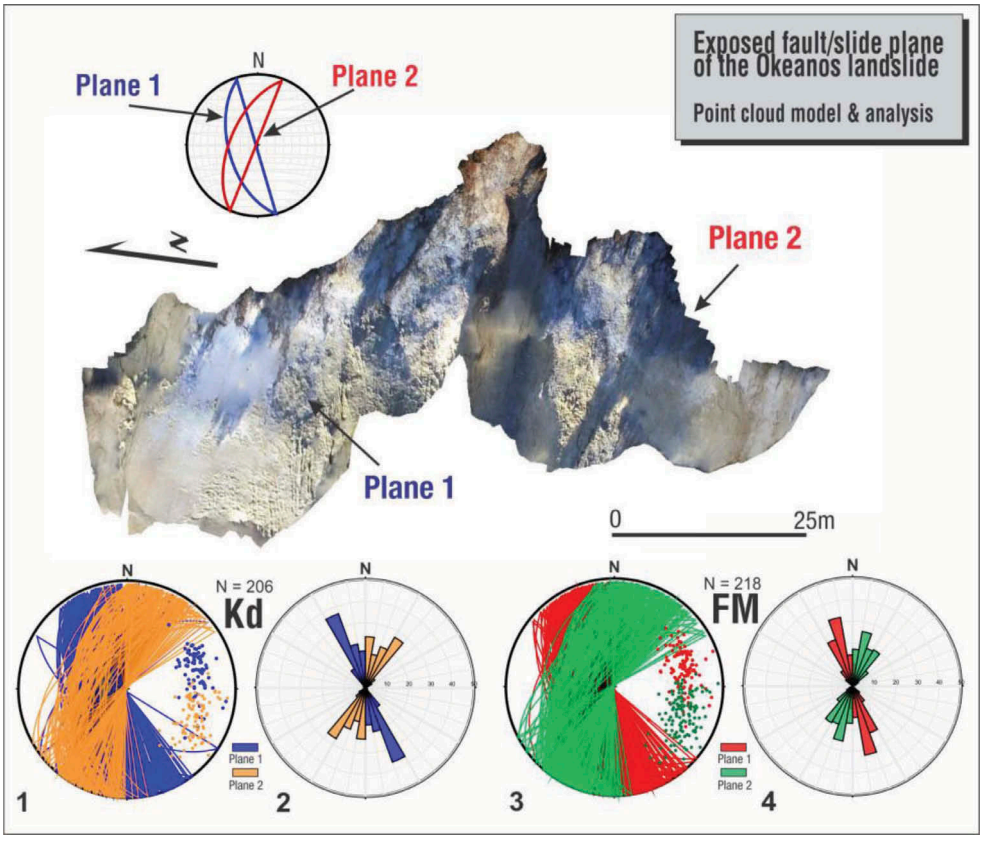

Figure 3. Structural analysis of the fault/slide plane of Okeanos landslide, using the point cloud dataset. Mean orientation of the two planes displayed on stereonet (lower-hemisphere projection). Bottom: Stereoplots and rose diagrams (strike) of the two fault planes using automatically extracted planar facets from the point cloud set using qFacets. Plots are made using the kd-tree (Kd) method (1 and 2) and using Fast Marching (FM) method (3 and 4).

wedge failure mechanism for the landslide, triggered by the strong ground motion of the earthquake. The two fault planes can be interpreted as either a local deviation (step) of the same fault surface or two conjugate faults in the form of R and P Riedel shears (angle 300°).

3 CASE STUDY OF 2017 KOS, GREECE EARTHQUAKE

The July 20, 2017 M6.6 earthquake triggered "typical" lateral spreading phenomena at the old harbor of the city of Kos. The earthquake ruptured a normal fault 10 km offshore Kos, dipping towards north (Ganas et al, 2017). This area was investigated in detail, during a post-earthquake field survey that took place on 13-14 August 2017, by performing traditional ground measurements as well as an image-based survey following the Structure from Motion (SfM) technique in order to virtually measure the deformation (Figure 1C). It should be pointed out that the applied SfM technique for measuring the lateral spreading displacement was based on a simple ground-based digital camera instead of a UAV (Papathanassiou et al, 2019).

In particular, 70 images of the displaced area were captured along a straight line that was perpendicular to the seashore and parallel to the direction of the spreading, in order to produce a SfM point cloud. The camera that was used on this post-earthquake reconnaissance survey was a Panasonic Lumix DMC-FZ18 of 8.1 megapixel resolution with an optical image stabilizer in the lens in order to reduce blurring by compensating for hand shake. Initial camera alignment was assisted by camera sensor GPS info and produced the original tie point set. The final point cloud was extracted by dense matching using ultra-high settings, for achieving the best resolution possible. Afterwards, a Digital Surface Model (DSM) of a 3 mm pixel size and orthomosaic were exported based on the dense point cloud.

A procedure suggested by Ishihara et al. (1997) and applied by Robinson et al. (2010) and Cubrinovski et al. (2012) in Christchurch, New Zealand and Franke et al. (2016) in Iquique, Chile in order to survey a lateral spreading was followed in this case study at Kos Island, Greece by Papathanassiou et al. (2019). In particular, along the line followed for the SfM-technique, the horizontal displacement (width of the cracks) and the vertical offset were measured at each location of failure (subsidence, cracks) using a surveyor's tape. Regarding the SfM technique, the point cloud obtained from the photogrammetric survey, was compared with a pre-earthquake ground surface profile (Figure 4).

Having developed the 3D point cloud, we were able to measure the cumulative width of cracks and the vertical displacements following the photogrammetric technique and compared them with

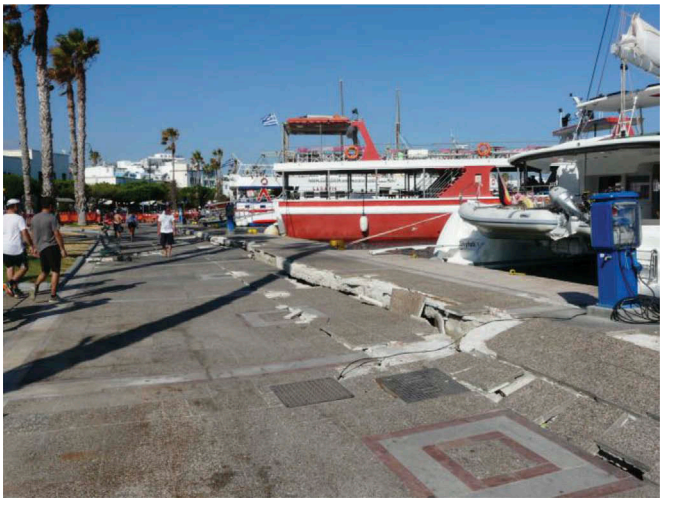

Figure 4a. Photo of the lateral spreading site analyzed in this study, located at the waterfront area of the city of Kos.

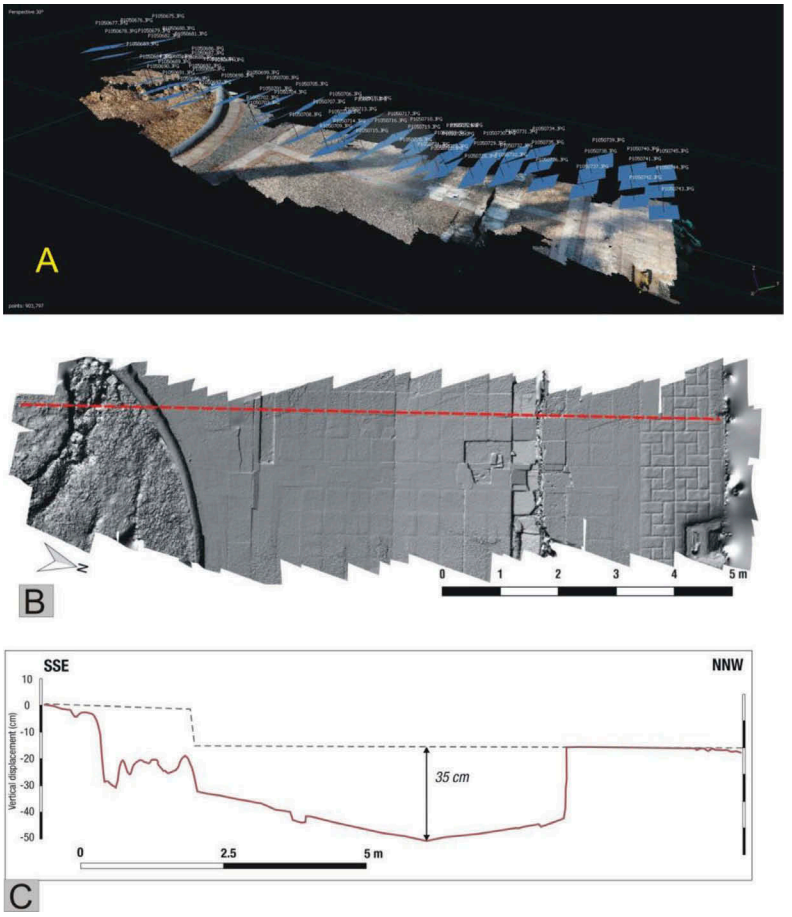

Figure 4. Creating a SfM model for the lateral spreading site in Kos site. A) Camera position and dense cloud created after image alignment and matching. B) Shaded relief map of the lateral spreading site. Red dotted line marks the location of profile C. C) Profile along the digital elevation model. Dotted line represents the pre-earthquake surface and red line the measured surface after the earthquake. Maximum measured vertical difference near the middle is 35 cm.

the ones obtained by the traditional field survey i.e. the manual measurements. In particular, the cumulative width of the cracks, measured based on SfM technique, is 1.114 m, and fits very well to the one measured by the traditional technique e.g. 1.104 m, less than 1% deviation. The deviation for the cumulative vertical offset is approximately 12%, which can be considered as significant. In particular, as it is pointed out by Papathanassiou et al. (2019), the cumulative offset measured based on SfM is 0.69 m, while the one measured using a surveyor's tape on the field is 0.61 m

4 CONCLUSION

Point clouds are suitable for performing structural geological measurements in addition or in the absence of field measurements. Various software packages permit the measurement of geological planes and orientations directly on the point cloud produced by UAV or LiDAR sensors. Using a point cloud, measurements can be made in inaccessible sites, while the larger number of measurements minimizes the statistical bias of the pattern of field measurements.

The use of the UAV system in the case of Okeanos landslide enabled the collection of essential information regarding the characteristics of the landslide. Extraction of a detailed point cloud enabled the high-resolution modeling of the landslide at a site with challenging conditions

such as limited accessibility and complex relief. Change analysis and volumetric calculation for co-seismic landslides demand a pre-event detailed point cloud set that can be co-registered and compared with the post-event set. Coastal areas are usually covered by multi-temporal aerial imagery in large scales that can be used to extract point clouds suitable as a reference.

In the case of Kos island, the SfM-based technique provides reliable data (on horizontal axis) regarding documenting and modeling lateral displacement features and accordingly, could be used for the purposes of a rapid post-earthquake field survey. Furthermore this technique can be applied even with a low cost ground-based technique e.g. a simple hand-held digital camera. However, the outcome arisen from the comparison of the measurements on vertical axis cannot be characterized as satisfactory, since a 12% deviation exists, and some caution should be applied when using this technique in order to measure vertical offset of fine features.

ACKNOWLEDGEMENTS

We acknowledge support of this research by the project "HELPOS - Hellenic Plate Observing System" (MIS 5002697) which is implemented under the Action "Reinforcement of the Research and Innovation Infrastructure", funded by the Operational Programme "Competitiveness, Entrepreneurship and Innovation" (NSRF 2014-2020) and co-financed by Greece and the European Union (European Regional Development Fund).

REFERENCES

Cubrinovski, M, Robinson, K, Taylor, M, Hughes, M, Orense, R. 2012. Lateral spreading and its impacts in urban areas in the 2010–2011 Christchurch earthquakes, New Zealand. J. Geol. Geoph. 55(3): 255-269.

Dewez, T.J.B., Girardeau-Montaut, D., Allanic, C., Rohmer, J.J., 2016. Facets: a CloudCompare plugin to extract geological planes from unstructured 3D point clouds. International Archives of the Photogrammetry, Remote Sensing and Spatial Information Sciences Vol.XLI-B5, doi:10.5194/isprsarchives-XLI-B5-799-2016

Franke, K, Rollins, K, Ledezma, C, Hedengren, J, Wolfe, D, Ruggles, S, Bender, C, Reimschiissel, B. 2016. Reconnaissance of Two Liquefaction Sites Using Small Unmanned Aerial Vehicles and Structure from Motion Computer Vision Following the April 1, 2014 Chile Earthquake. J. Geot. Geoenvir. Engin. 143 (5) 04016125-1-11.

Ganas, A., Elias, P., Bozionelos, G., Papathanassiou, G., Avallone, A., Papastergios, A., Valkaniotis, S., Parcharidis, Is., Briole, P., 2016. Coseismic deformation, field observations and seismic fault of the 17 November 2015 M=6.5, Lefkada Island, Greece earthquake, Tectonophysics 687; 210-222 http://dx.doi.org/10.1016/j.tecto.2016.08.012

Ganas, A., P. Elias, S. Valkaniotis, P. Briole, V. Kapetanidis, I. Kassaras, A. Barberopoulou, P. Argyrakis, G. Chouliaras, A. Moshou, 2017. Co-seismic deformation and preliminary fault model of the July 20, 2017 M6.6 Kos earthquake, Aegean Sea. Report submitted to EMSC on 30 July 2017, 20 pages https://www.emsc-csem.org/Files/event/606346/Kos_report_30-7-2017.pdf

Ishihara, K, Yoshida, K, Kato, M. 1997. Characteristics of lateral spreading in liquefied deposits during the 1995 Hanshin-Awaji earthquake. J Earthq Engin. 1(1):23-55.

Lague, D., Brodu, N., Leroux, J., 2013. Accurate 3D comparison of complex topography with terrestrial laser scanner: application to the Rangitikei canyon (N-Z). ISPRS J. Photogramm. Remote Sens. 82; 10–26.

Papathanassiou, G., Valkaniotis, S., Ganas, A., Grendas, N., Kollia, E. 2017. The November 17th, 2015 Lefkada (Greece) strike-slip earthquake: Field mapping of generated failures and assessment of macroseismic intensity ESI-07. Engineering Geology 220; 13-30.

Papathanassiou, G., Valkaniotis, S., Pavlides, S. 2019. The July 20, 2017 Bodrum-Kos, Aegean Sea Mw=6.6 earthquake; preliminary field observations and image-based survey on a lateral spreading site. Soil Dyn. Earth. Engin. 116; 668-680.

Robinson, K, Cubrinovski, M, Kailey, P, Orense, R. 2010. Field measurements of lateral-spreading following the 2010 Darfield earthquake. Proceedings of 9th Pacific Conference on Earthquake Engineering, 14_16 April, Auckland 2011 Paper No. 52: 1_8. 2010.

Valkaniotis, S., Papathanassiou, G., Ganas, A. 2018. Mapping an earthquake-induced landslide based on UAV imagery; case study of the 2015 Okeanos landslide, Lefkada, Greece. Engineering Geology 245, 141-152.